Total and partial shear viscosity in heavy-ion collisions at intermediate energies

E. Zabrodin,

in collaboration with

M. Teslyk and L. Bravina

XI-th International Conference on New Frontiers in Physics ICNFP-2022

Kolymbari, Crete, Greece, 30.08-11.09.2022

Motivation

Search for critical point

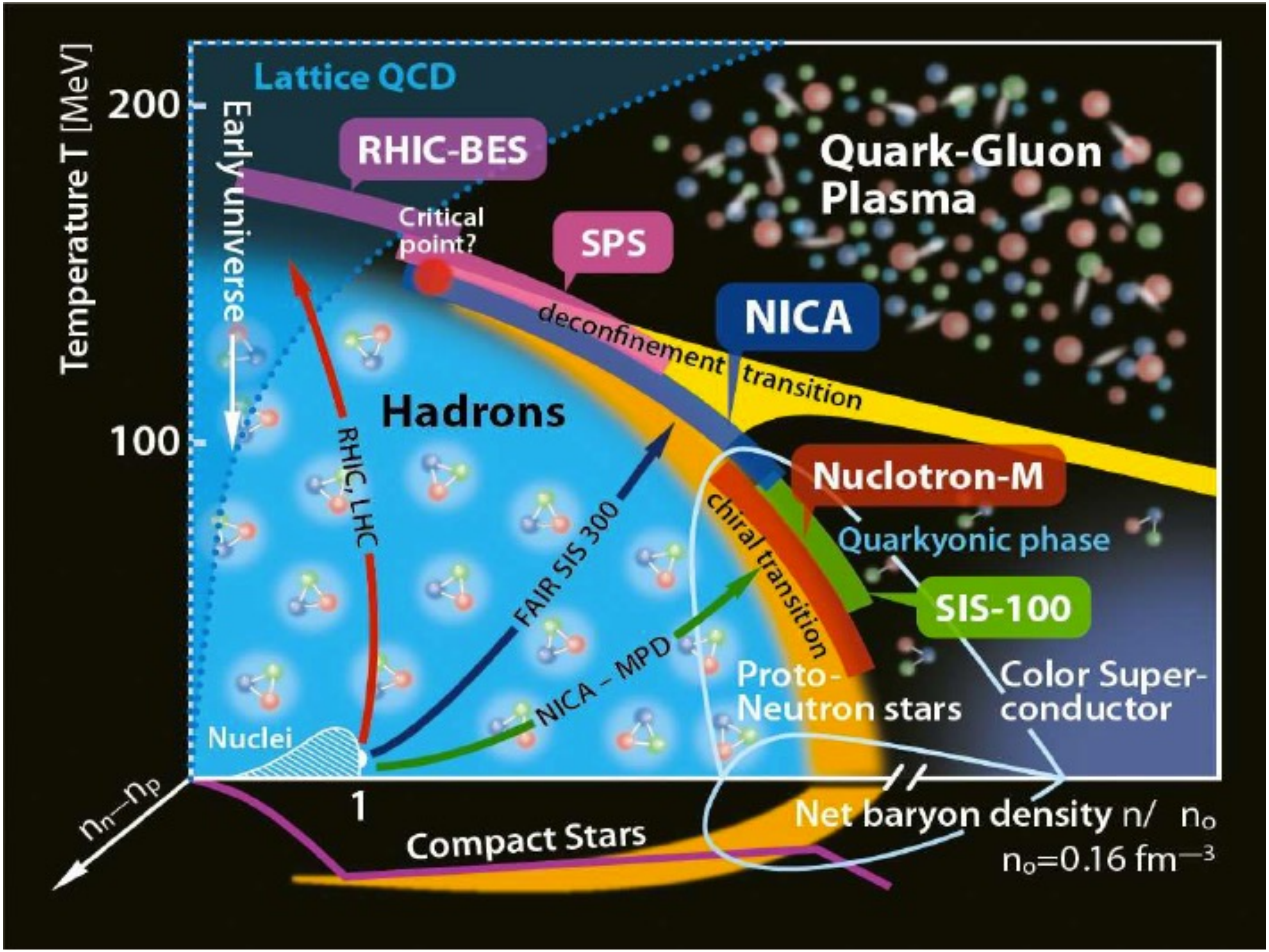

Temperature T [MeV]
200
100
Lattice QCD
Early universe
RHIC-BES
Critical point?
SPS
Quark-Gluon Plasma
NICA
deconfinement transition
Hadrons
RHIC, LHC
FAIR SIS 300
NICA – MPD
chiral transition
Nuclotron-M
Quarkyonic phase
SIS-100
Proto-Neutron stars
Color Super-conductor
Nuclei
1
$n_n - n_p$
Compact Stars
Net baryon density n/n_0
n_0=0.16 fm^{-3}

Motivation

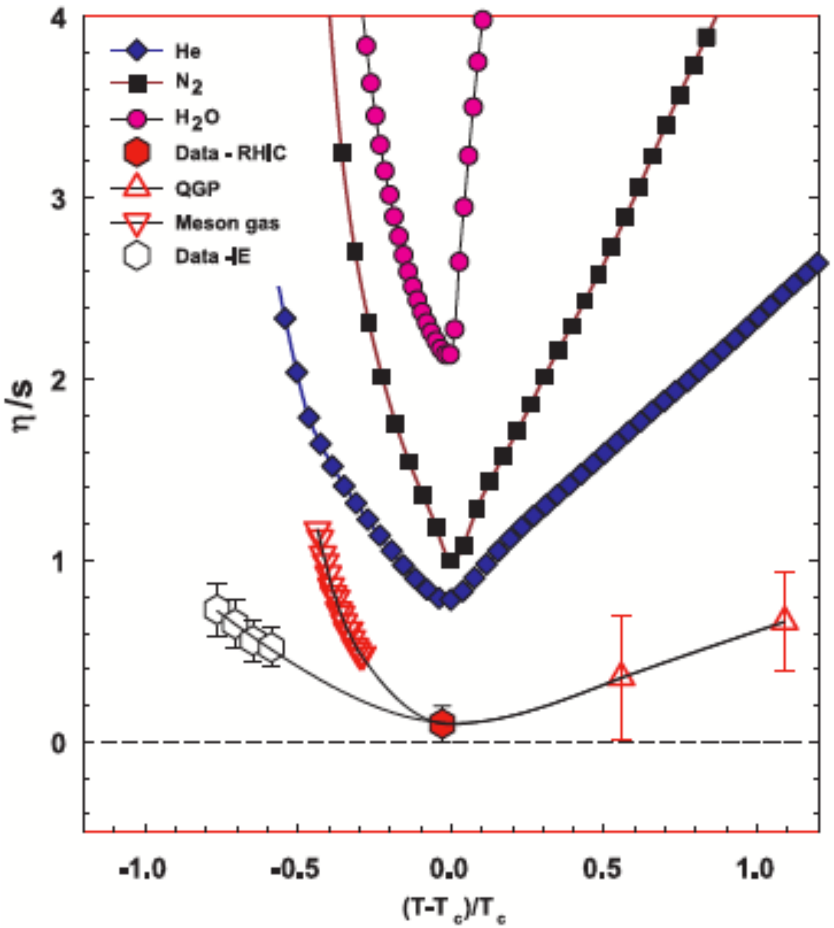

courtesy of R.Lacey & A.Taranenko

P.Kovtun, D.Son, A.Starinets, PRL 94 (2005) 111601

$$\frac{\eta}{s} \geq \frac{1}{4\pi}$$

- A.Muronga. PRC 69, 044901 (2004)
- L.Csernai, J.Kapusta, L.McLerran. PRL 97, 152303 (2006)
- P.Romatschke, U.Romatschke. PRL 99, 172301 (2007)
- S.Plumari et al. PRC 86, 054902 (2012)
- ALICE collaboration, CERNCOURIER (14.10.2016)
- J.Rose et al. PRC 97, 055204 (2018)

For all known substances the ratio of shear viscosity to entropy density reaches a minimum at critical temperature

Motivation

U.Heinz, R. Snellings, Ann.Rev.Nucl.Part.Sci. 63 (2013) 123

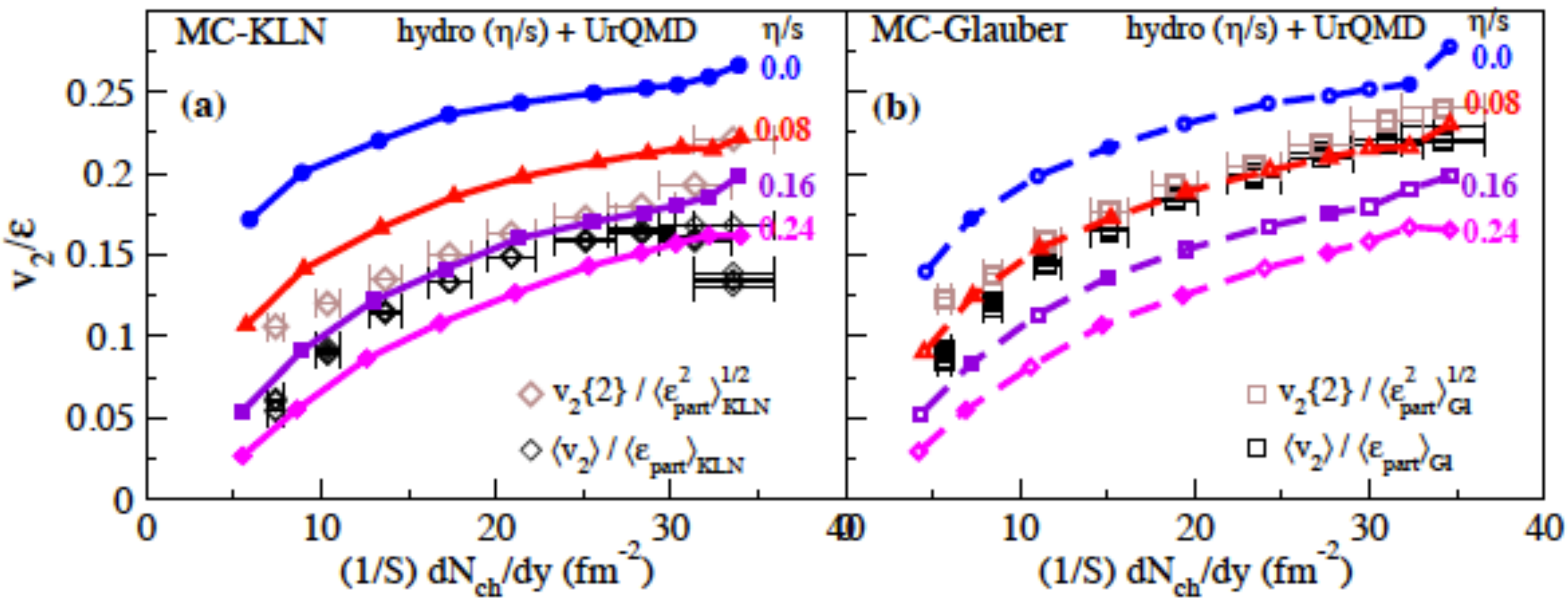

The theoretical curves are calculated with the VISHNU model for different (temperature-independent) choices of the specific QGP shear viscosity $\frac{\eta}{s}$.
It is necessary to decribe the STAR data on elliptic flow in Au+Au @ 200 GeV

Theory

Green-Kubo: shear viscosity η may be defined as:

$$\eta(t_0) = \frac{1}{\hbar}\frac{V}{T}\int_{t_0}^{\infty} \mathrm{d}t \langle \pi(t)\pi(t_0)\rangle_t = \boxed{\frac{\tau}{\hbar}\frac{V}{T}\langle \pi(t_0)\pi(t_0)\rangle,}$$

where

$$\langle \pi(t)\pi(t_0)\rangle_t = \frac{1}{3}\sum_{\substack{i,j=1\\ i\neq j}}^{3} \lim_{t_{\max}\to\infty} \frac{1}{t_{\max}-t_0}\int_{t_0}^{t_{\max}} \mathrm{d}t' \pi^{ij}(t+t')\pi^{ij}(t')$$

$$= \langle \pi(t_0)\pi(t_0)\rangle \exp\left(-\frac{t-t_0}{\tau}\right)$$

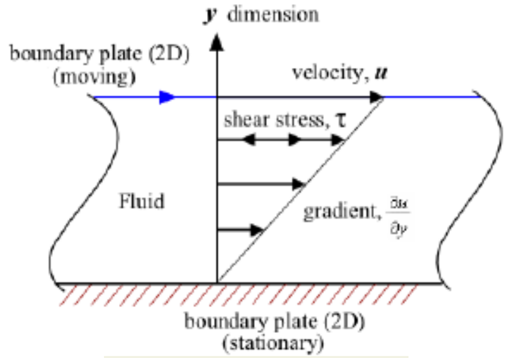

$$T_{xy} = -\eta\frac{\partial u_x}{\partial y}$$

with

$$\pi^{ij}(t) = \frac{1}{V}\sum_{\text{particles}} \frac{p^i(t)\,p^j(t)}{E(t)}$$

t_0: initial cut-off time to start with

Models:

UrQMD, Box, Stat.M

Initial Particle Production in UrQMD

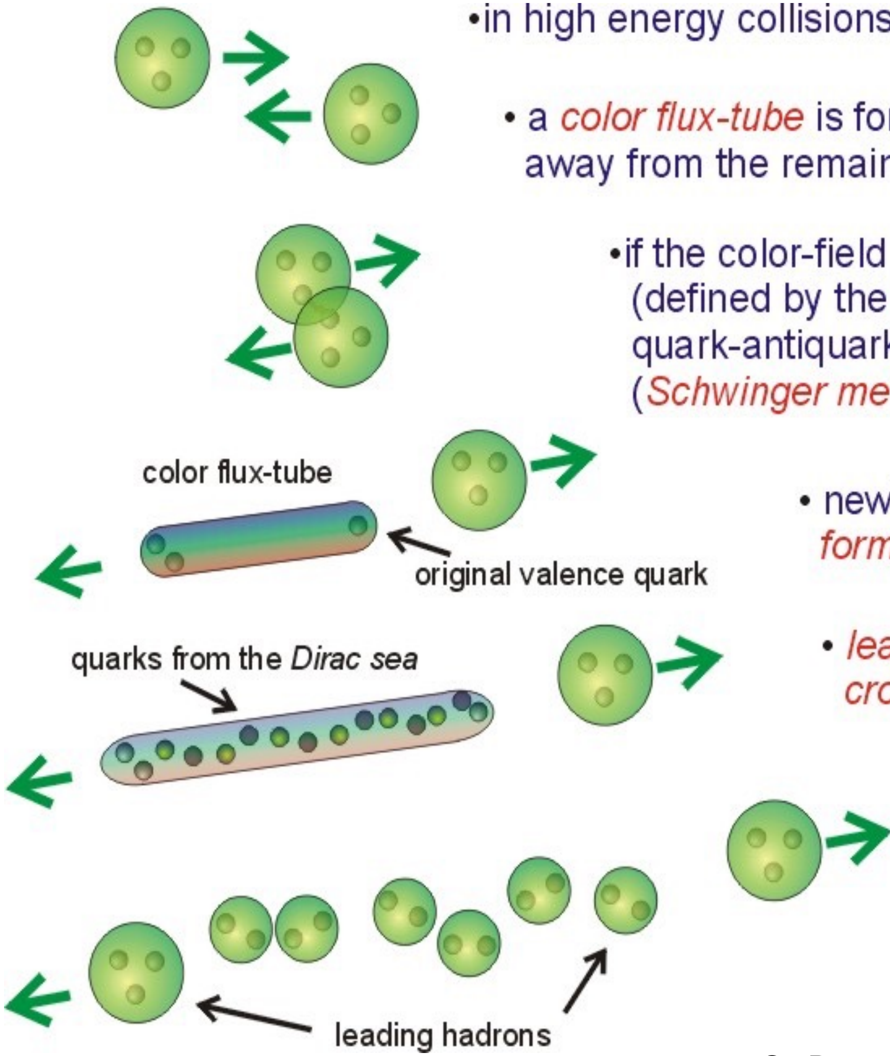

- in high energy collisions hadrons can be excited into *strings*
- a *color flux-tube* is formed by pulling one valence quark away from the remaining ones in the hadron
- if the color-field increases beyond a critical value (defined by the *string-tension*), spontaneous quark-antiquark creation from the *Dirac sea* occurs (*Schwinger mechanism*)
- newly created (anti-)quarks require a *formation time* to form hadrons
- *leading hadrons* interact with *reduced cross sections* during their formation time
- *newly created hadrons* have *zero cross section* during their formation time

S. Bass et al., Prog.Part.Nucl.Phys. 41 (1998) 255
M. Bleicher, E.Z., et al., J.Phys.G 25 (1999) 1859

Box with periodic boundary conditions

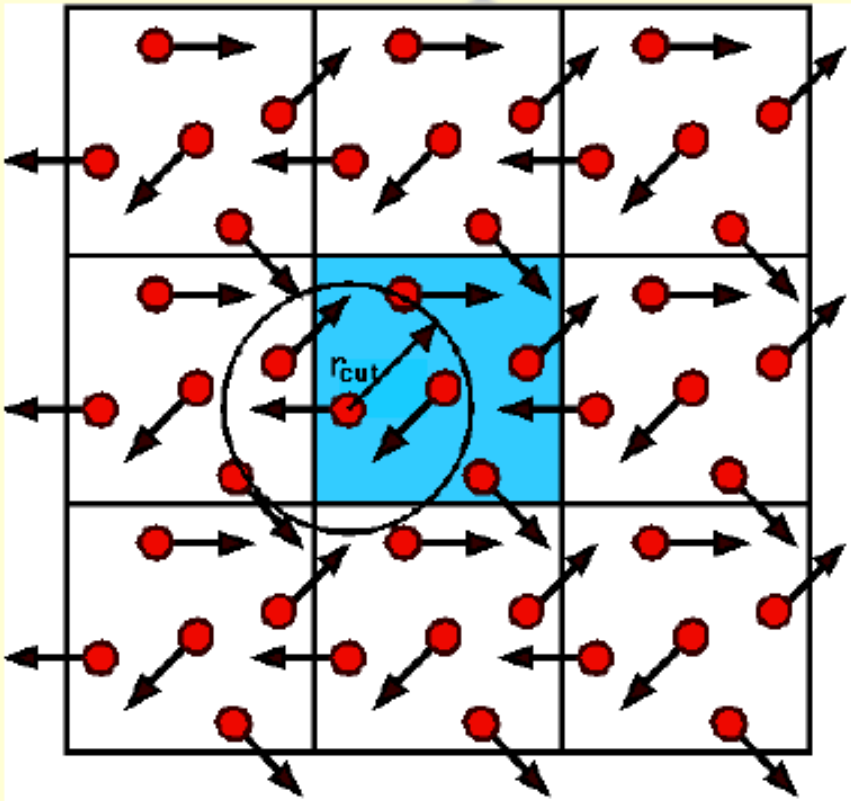

M.Belkacem et al., PRC 58, 1727 (1998)

Initialization: (i) nucleons are uniformly distributed in a configuration space;
(ii) Their momenta are uniformly distributed in a sphere with random radius and then rescaled to the desired energy density.

Model employed: UrQMD
55 different baryon species (N, Δ, hyperons and their resonances with $m \leq 2.25\ GeV/c^2$)
32 different meson species (including resonances with $m \leq 2\ GeV/c^2$) and their respective antistates.
For higher mass excitations a string mechanism is invoked.

Test for equilibrium: particle yields and energy spectra

Equilibration in the Central Cell

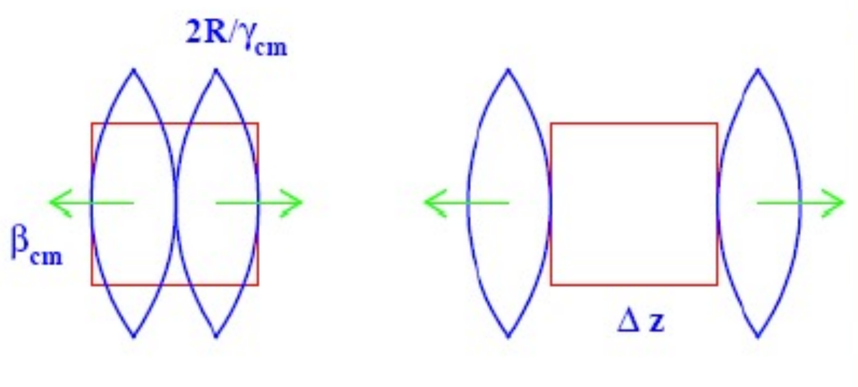

$t^{cross} = 2R/(\gamma_{cm}\,\beta_{cm})$ $\quad$ $t^{eq} \geq t^{cross} + \Delta z/(2\beta_{cm})$

Kinetic equilibrium:

Isotropy of velocity distributions

Isotropy of pressure

Thermal equilibrium:

Energy spectra of particles are described by Boltzmann distribution

L.Bravina et al., PLB 434 (1998) 379; JPG 25 (1999) 351

$$\frac{dN_i}{4\pi p E dE} = \frac{V g_i}{(2\pi\hbar)^3} \exp\left(\frac{\mu_i}{T}\right) \exp\left(-\frac{E_i}{T}\right)$$

Chemical equlibrium:

Particle yields are reproduced by SM with the same values of $(T,\ \mu_B,\ \mu_S)$:

$$N_i = \frac{V g_i}{2\pi^2\hbar^3} \int_0^\infty p^2 dp \exp\left(\frac{\mu_i}{T}\right) \exp\left(-\frac{E_i}{T}\right)$$

Statistical model of ideal hadron gas

input values

output values

$$\varepsilon^{\mathrm{mic}} = \frac{1}{V}\sum_i E_i^{\mathrm{SM}}(T,\mu_{\mathrm{B}},\mu_{\mathrm{S}}),$$

$$\rho_{\mathrm{B}}^{\mathrm{mic}} = \frac{1}{V}\sum_i B_i \cdot N_i^{\mathrm{SM}}(T,\mu_{\mathrm{B}},\mu_{\mathrm{S}}),$$

$$\rho_{\mathrm{S}}^{\mathrm{mic}} = \frac{1}{V}\sum_i S_i \cdot N_i^{\mathrm{SM}}(T,\mu_{\mathrm{B}},\mu_{\mathrm{S}}).$$

Multiplicity

Energy

Pressure

Entropy density

$$N_i^{\mathrm{SM}} = \frac{V g_i}{2\pi^2\hbar^3}\int_0^\infty p^2 f(p,m_i)dp,$$

$$E_i^{\mathrm{SM}} = \frac{V g_i}{2\pi^2\hbar^3}\int_0^\infty p^2\sqrt{p^2+m_i^2}\, f(p,m_i)dp$$

$$P^{\mathrm{SM}} = \sum_i \frac{g_i}{2\pi^2\hbar^3}\int_0^\infty p^2 \frac{p^2}{3(p^2+m_i^2)^{1/2}}\, f(p,m_i)dp$$

$$s^{\mathrm{SM}} = -\sum_i \frac{g_i}{2\pi^2\hbar^3}\int_0^\infty f(p,m_i)\,[\ln f(p,m_i) - 1]\, p^2 dp$$

Calculation of

Shear viscosity

M. Teslyk et al., Phys. Rev. C 101 (2020) 014904
E. Zabrodin et al., Phys. Scr. 85 (2020) 074009
E. Zabrodin et al., Nucl. Phys. A 1005 (2021) 121861

Evolution of temperature T and energy density ε

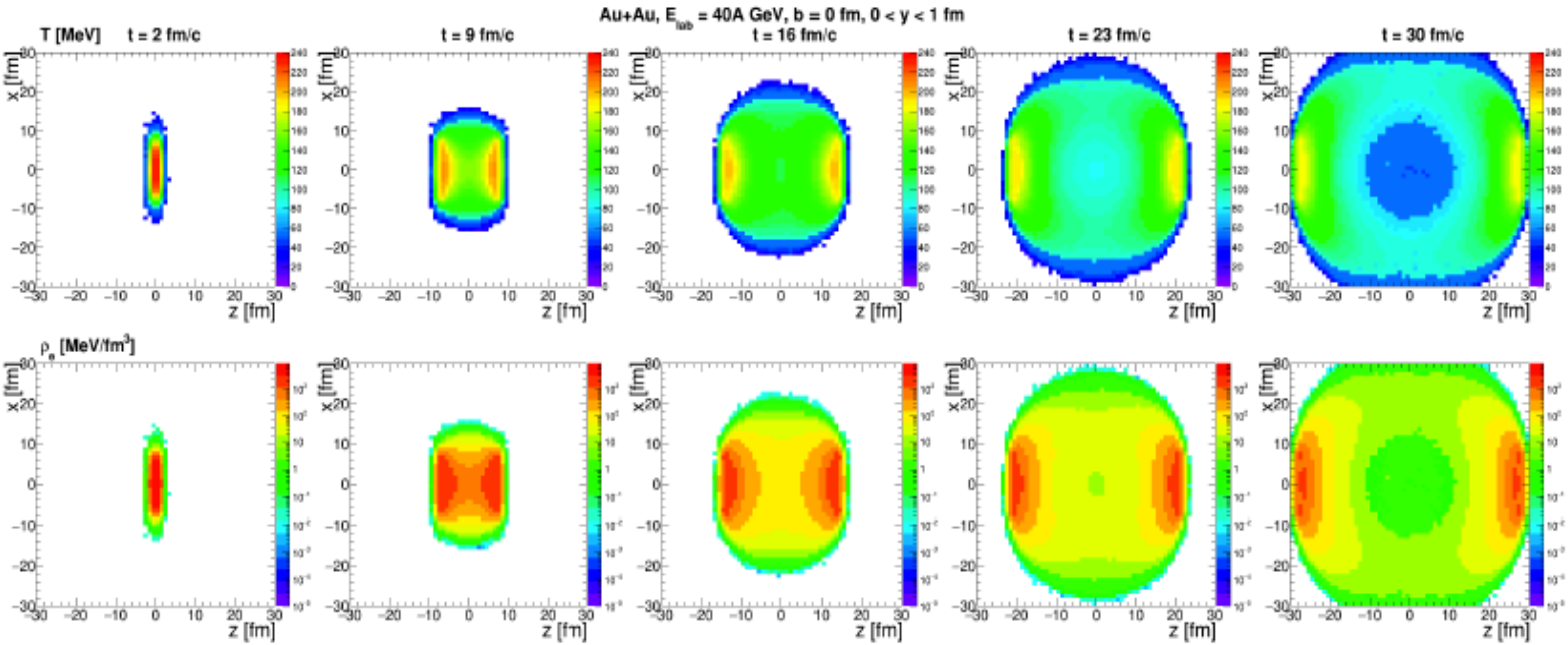

There is no global equilibrium in the whole volume of the fireball.
We opted for the central cell with volume $V = 5\times5\times5 = 125\ fm^3$

Evolution of baryon chemical potential μ_B and net-baryon density ρ_B

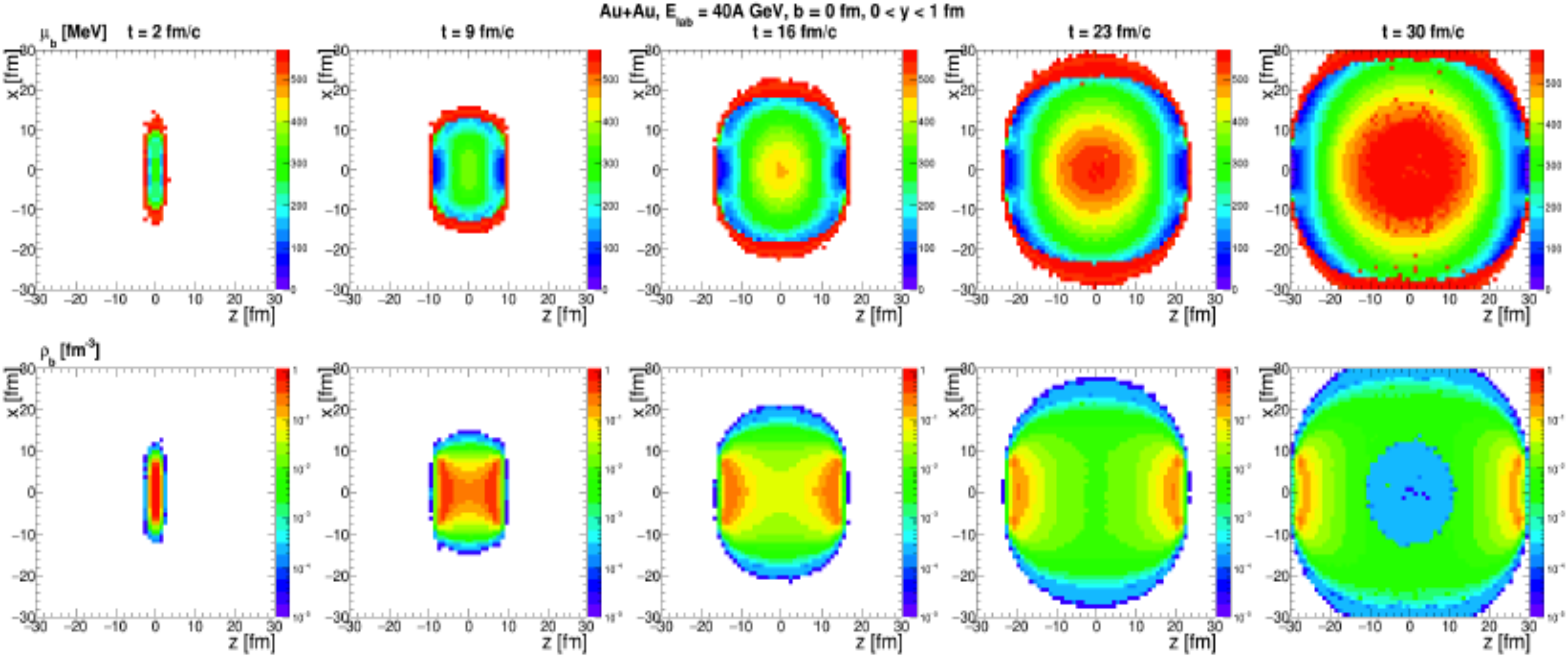

Net-baryon density is non-uniformly distributed within the whole volume, therefore baryon chemical potential is also different in different areas

Evolution of strangeness chemical potential μ_S and net-strangeness density ρ_S

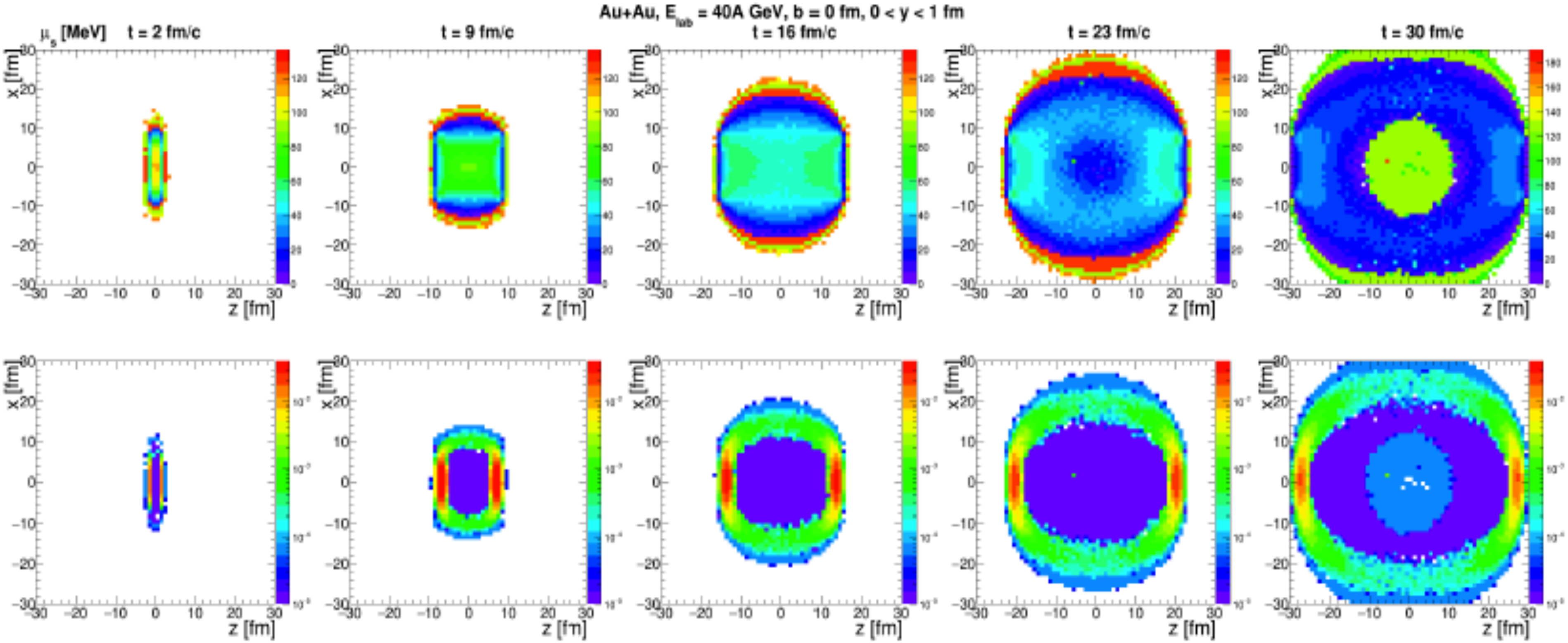

Net-strangeness density is also non-uniformly distributed within the whole volume.
Net-strangeness chemical potential is different in different areas

Cell + SM

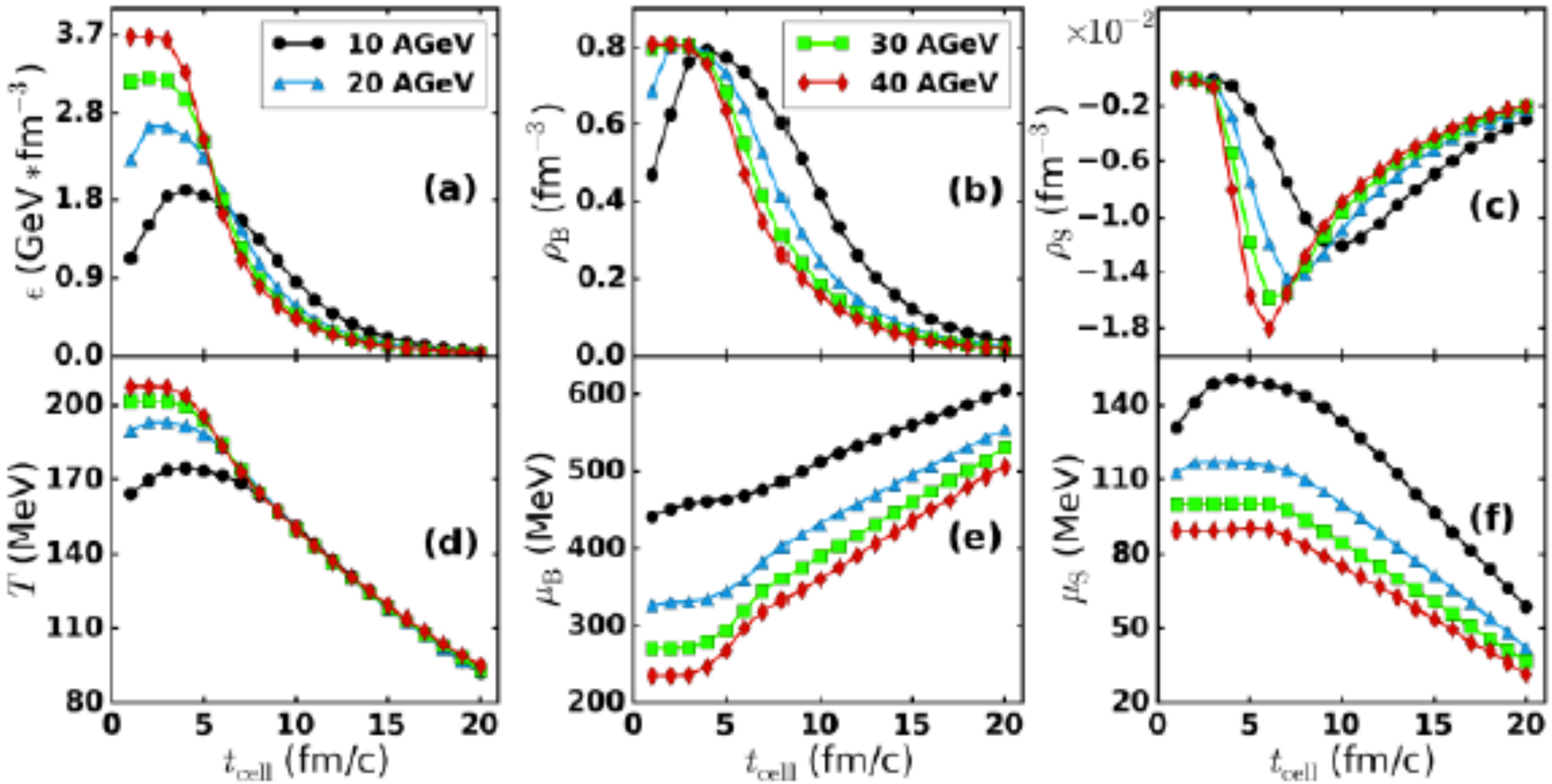

Dependence of $\varepsilon, \rho_B, \rho_S$ (from cell) and of T, μ_B, μ_S (from SM) on t_{cell}

Results: $\langle \pi(t)\,\pi(t_0) \rangle_t$ at $E \in [10, 20, 30, 40]$ AGeV

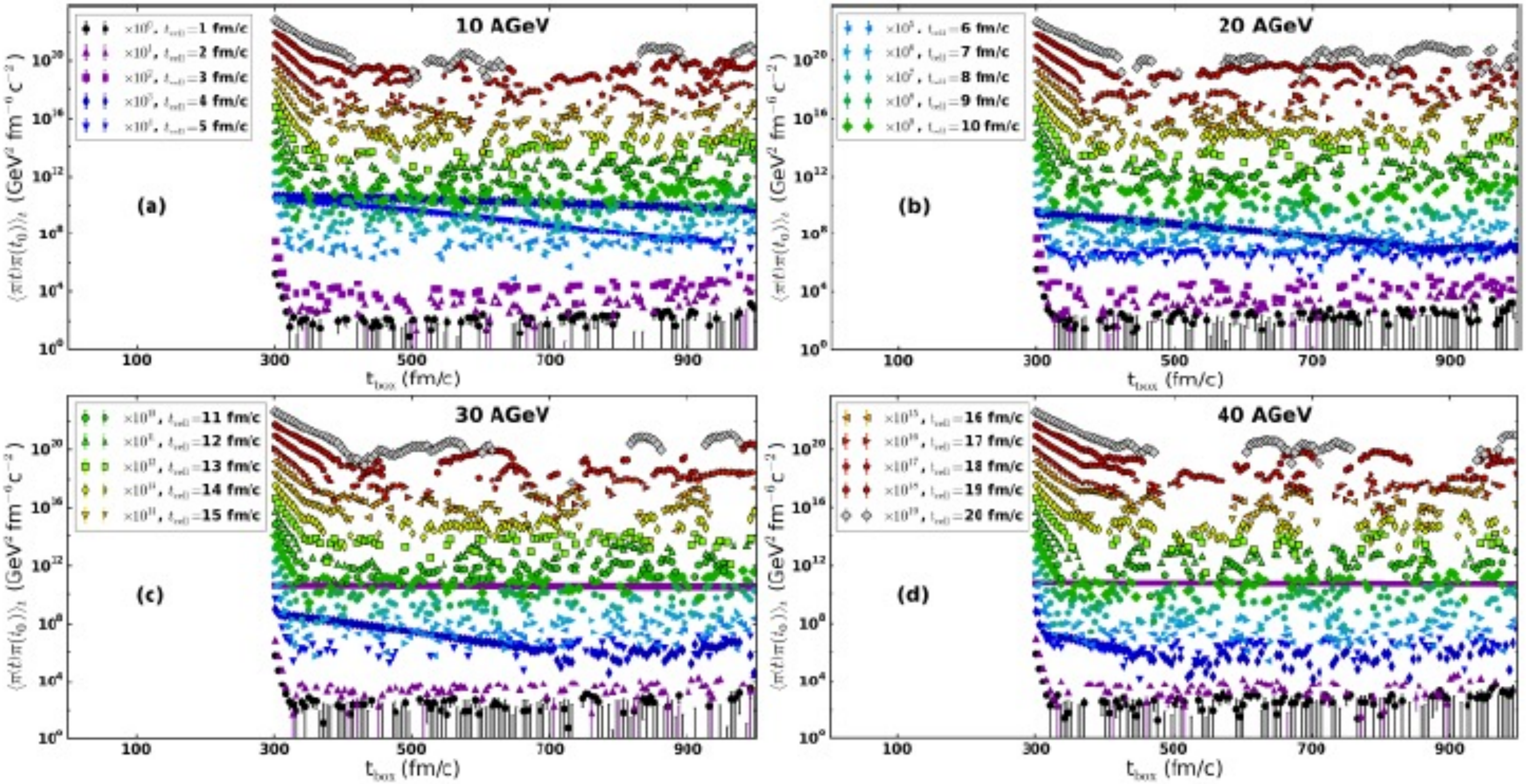

Time dependence of correlators $\langle \pi(t)\,\pi(t_0) \rangle_t$

$t_0 = 300$ fm/c

$t_{\text{cell}} \in \{1 \div 20\}$ fm/c

M. Teslyk, L. Bravina, …, E. Zabrodin, PRC 101 (2020) 014904

Results: $\langle \pi(t)\,\pi(t_0)\rangle_t$ at fixed t_{cell}

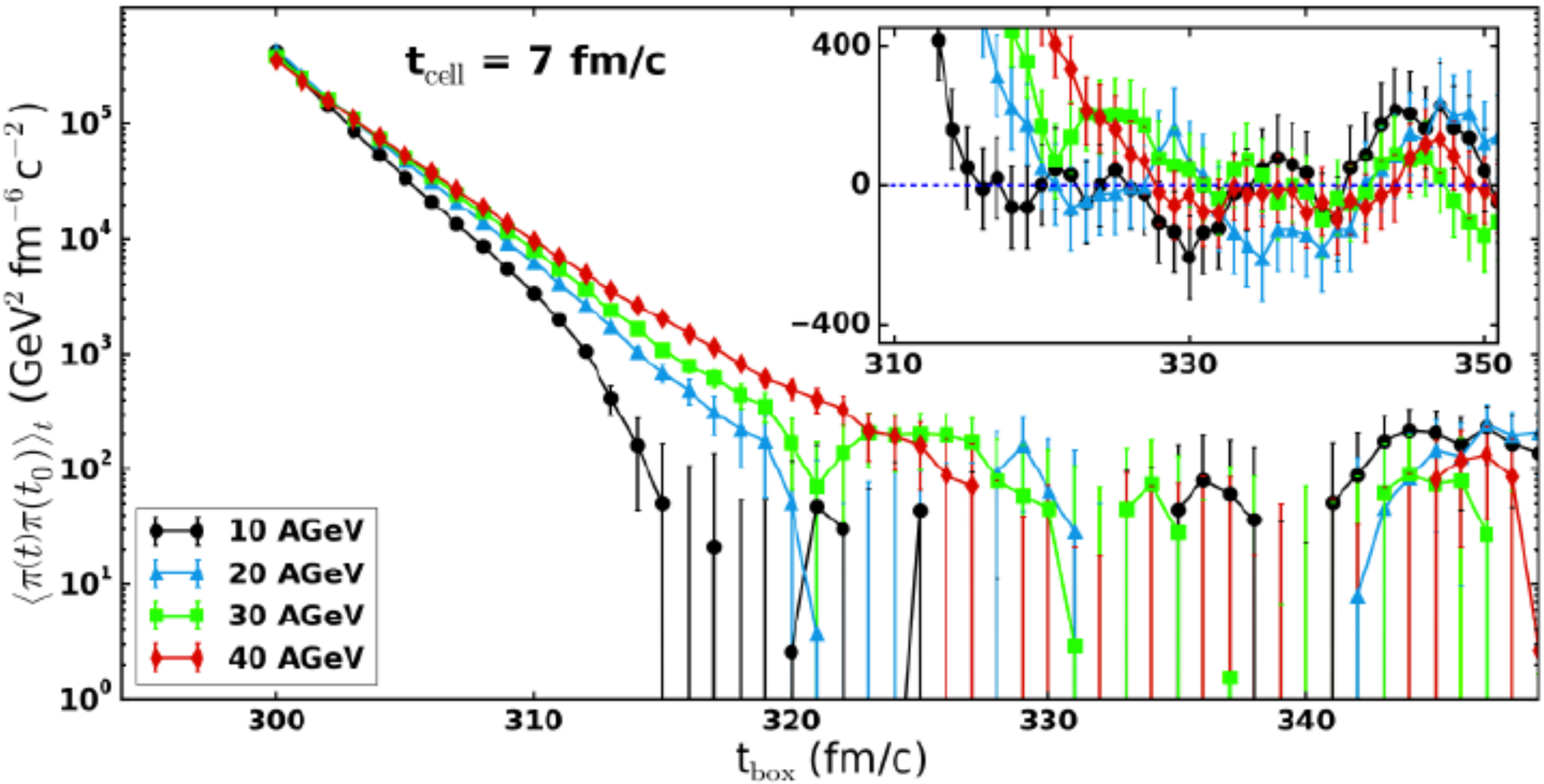

Time dependence of correlators $\langle \pi(t)\,\pi(t_0)\rangle_t$

Subplot: the same but at linear scale

$t_0 = 300$ fm/c

$t_{\mathrm{cell}} = 7$ fm/c

Results: τ from the fit

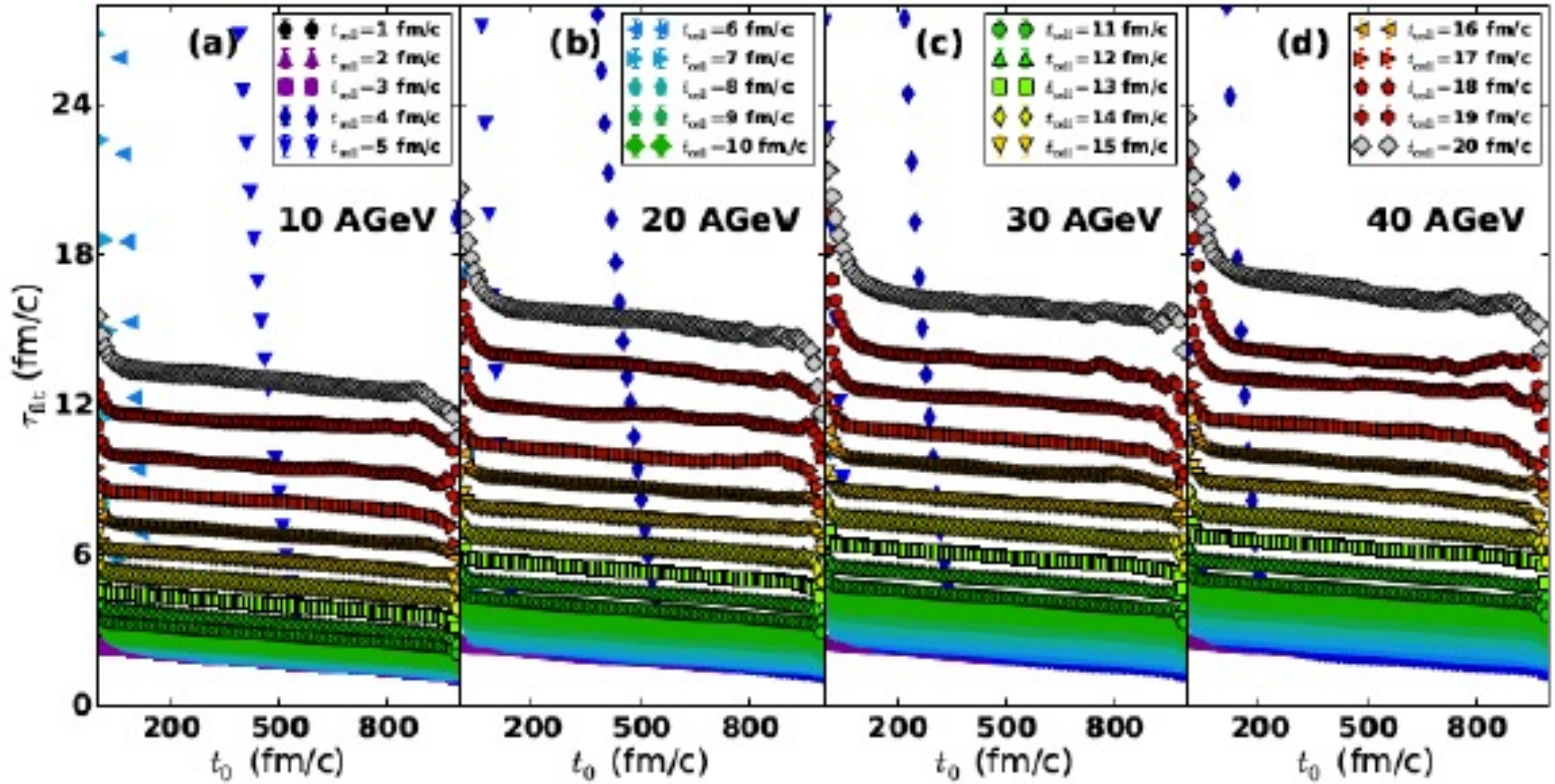

Dependence of τ_{fit} on t_0

Results: viscosity $\eta\,(t_{\text{cell}})$

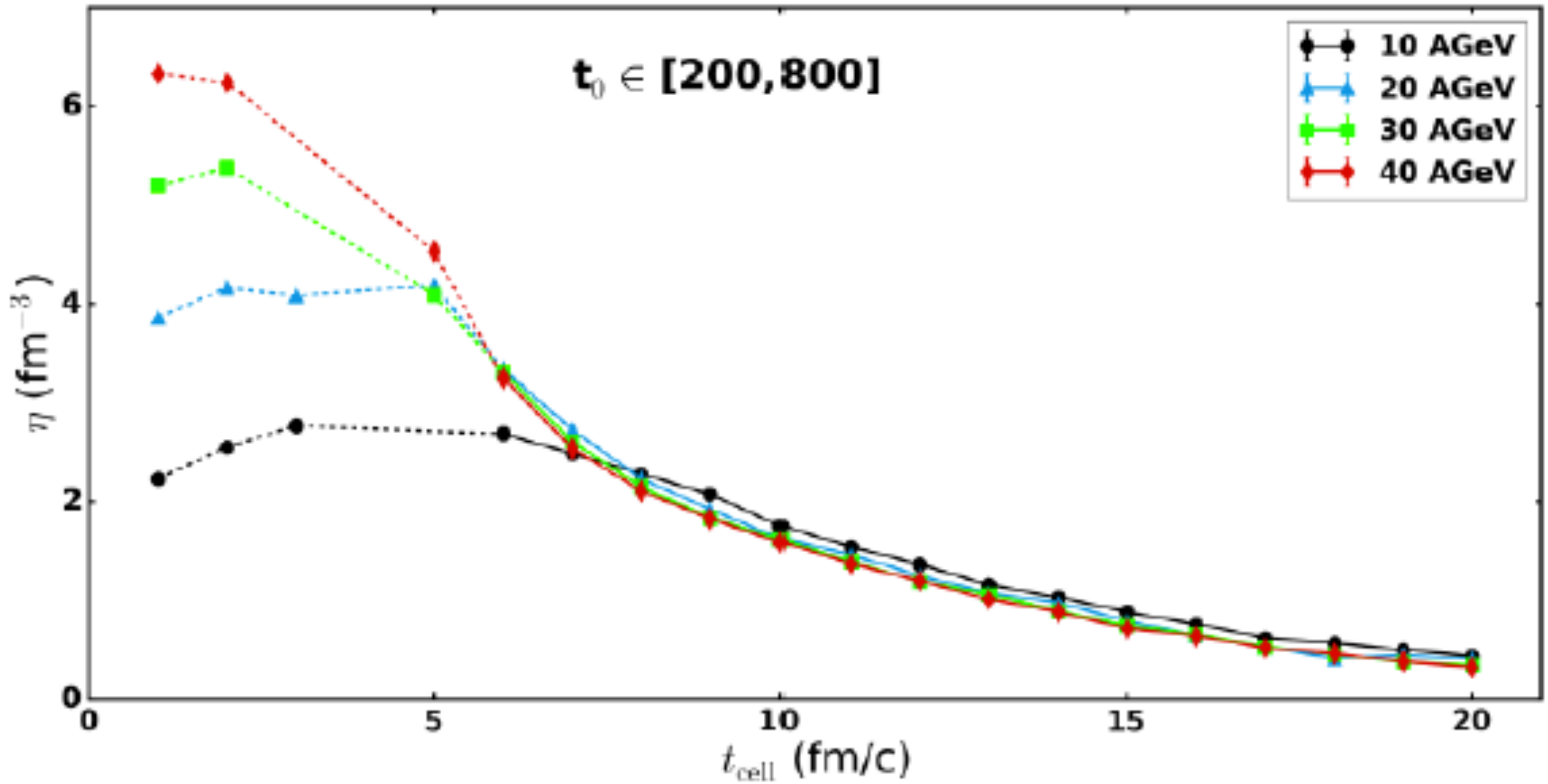

Dynamics of η in cell
All curves sit on the top of each other for $t_{\text{cell}} \geq 7$ fm/c

Results: η/s

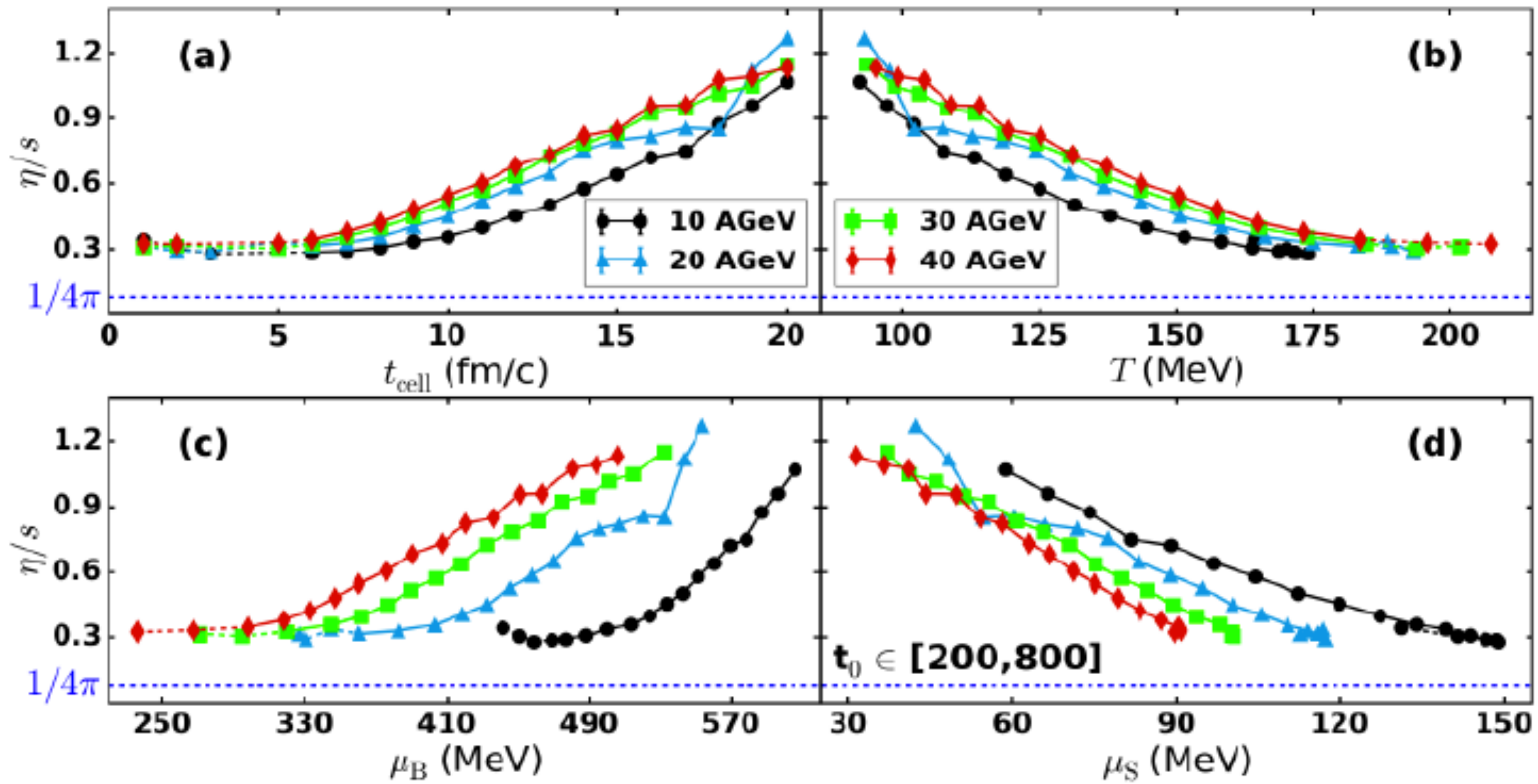

Dynamics of η/s in cell
as function of time, T, μ_{B}, μ_{S}

Calculation of

Partial η

M. Teslyk, L. Bravina, E. Zabrodin, Symmetry 14 (2022) 634

Results: viscosity $\eta\,(t_{\text{cell}})$

Nucleons

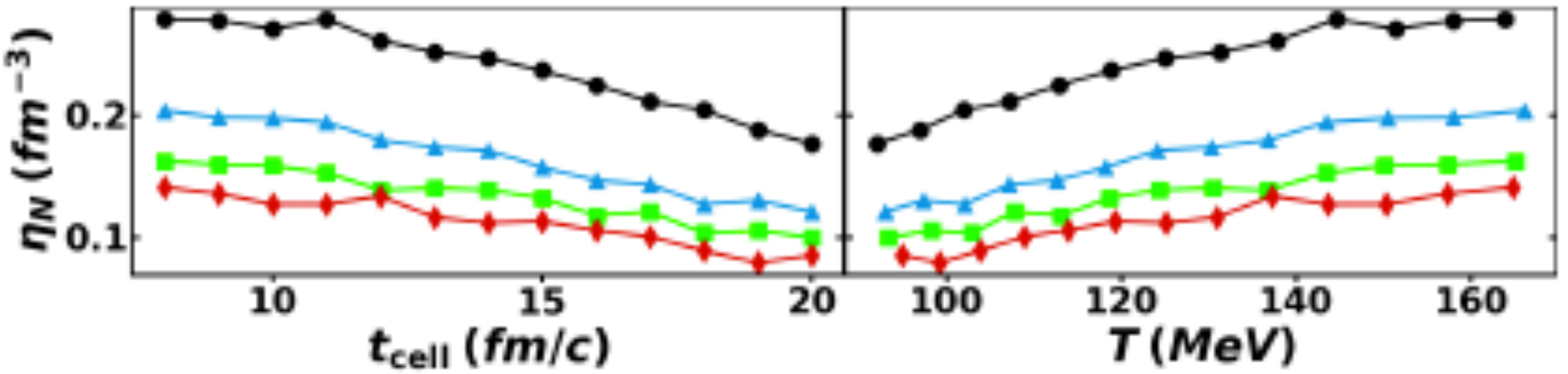

$\Lambda + \Sigma$

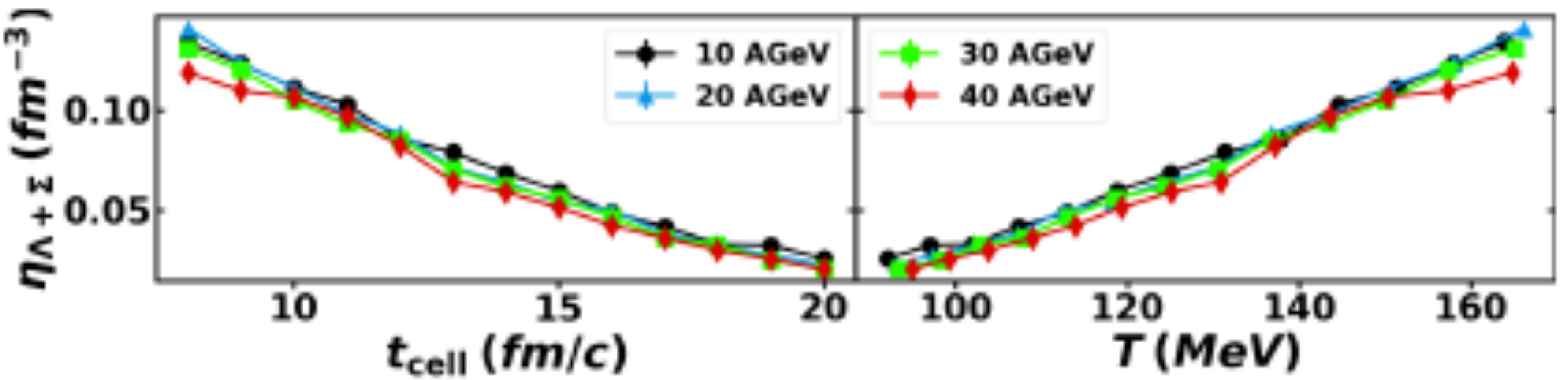

The lower the energy of nuclear collision, the higher the nucleon's shear viscosity. The values of shear viscosity of $\Lambda + \Sigma$ are close to each other. These values are almost two times lower compared to those of nucleons.

Results: viscosity $\eta\,(t_{\mathrm{cell}})$

Pions

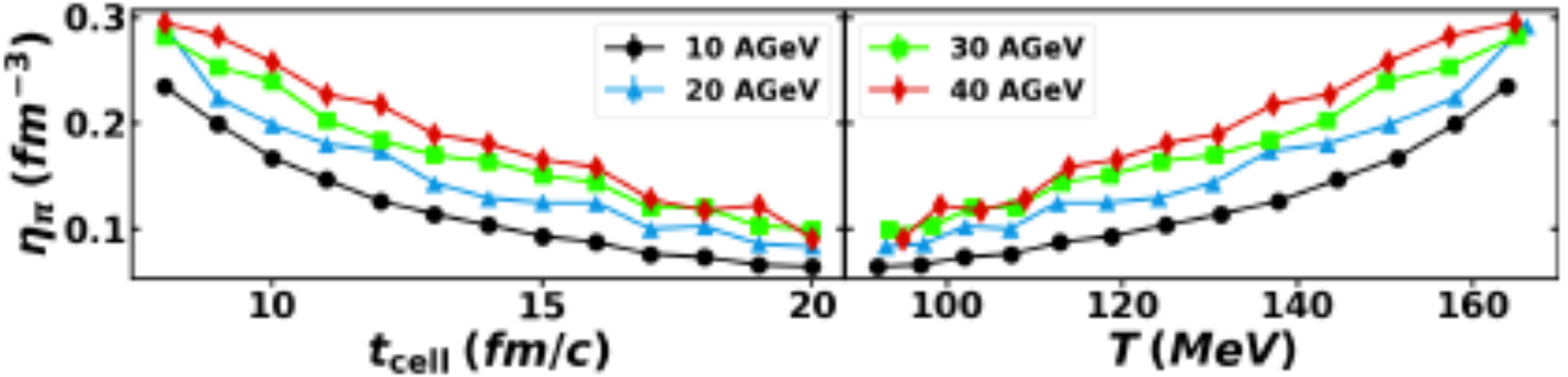

Kaons

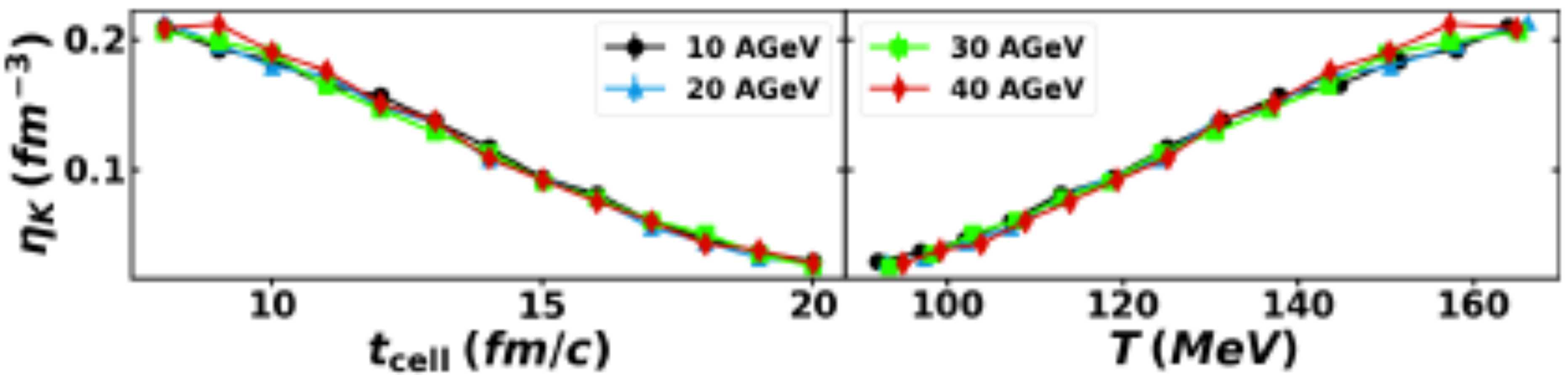

The lower the energy of nuclear collision, the lower the pion's shear viscosity. The values of shear viscosity of kaons sit on the top of each other.

Results: η / s_{SM}

More distributions:

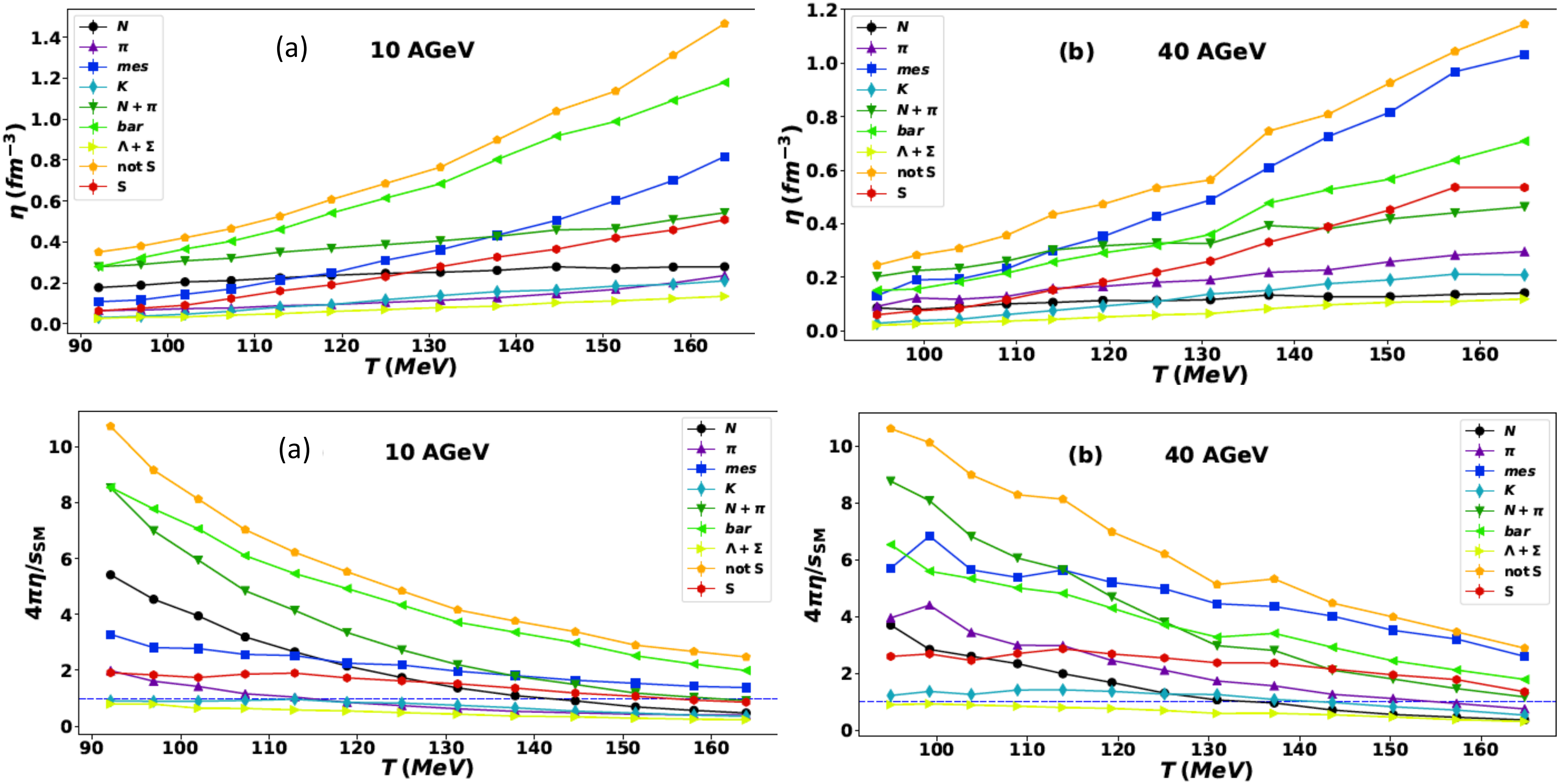

At E_{lab} = 10 AGeV shear viscosity of baryons is larger than that of mesons, whereas at E_{lab} = 40 AGeV mesons start to dominate

Results: viscosity $\eta\,(t_{\mathrm{cell}})$

Baryons

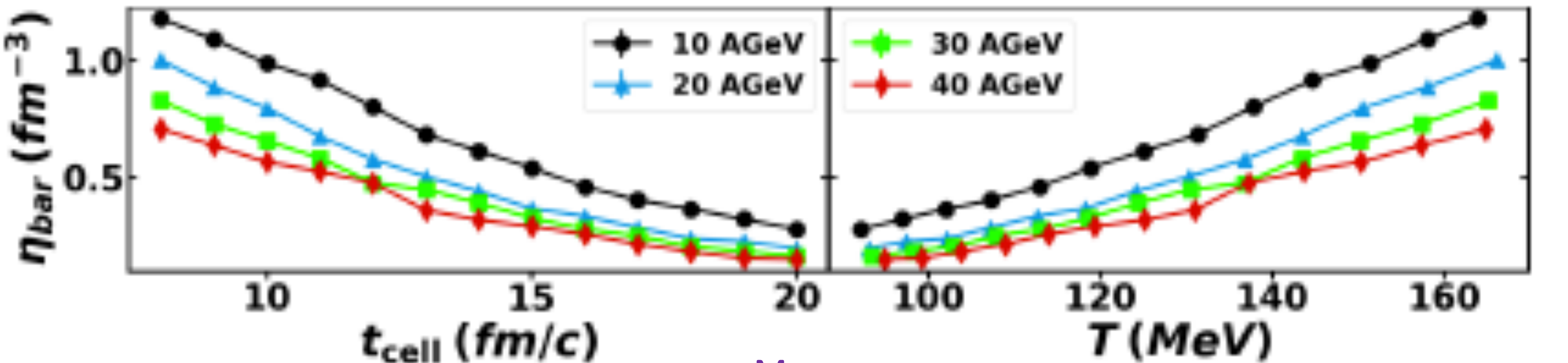

Mesons

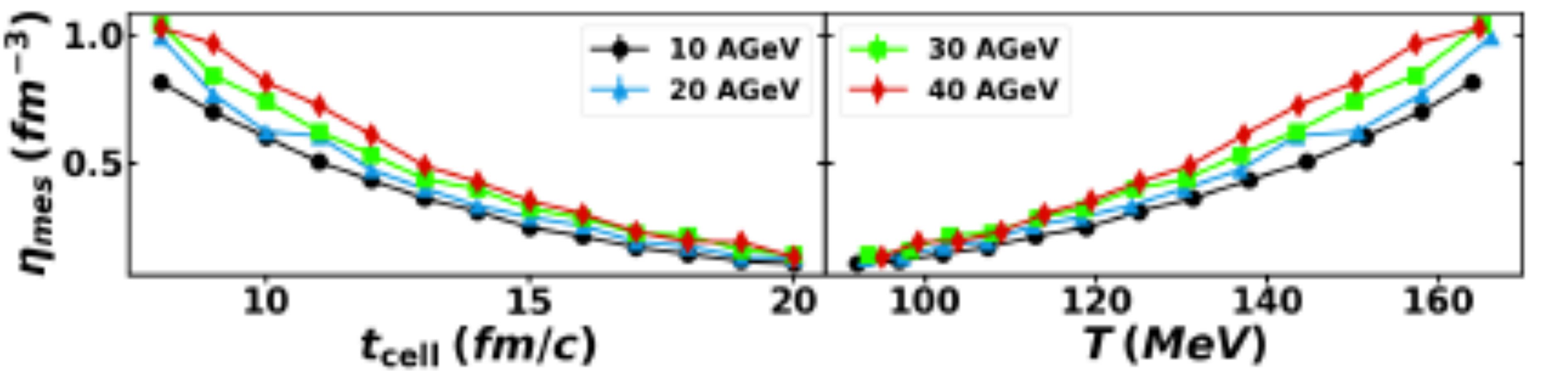

Shear viscosity of both baryons and mesons drops with time, i.e., with the reduction of T and ε .
However, η_B increases with decreasing $\sqrt{s}$, whereas η_M decreases.

Results: η/s_{SM}

Baryons

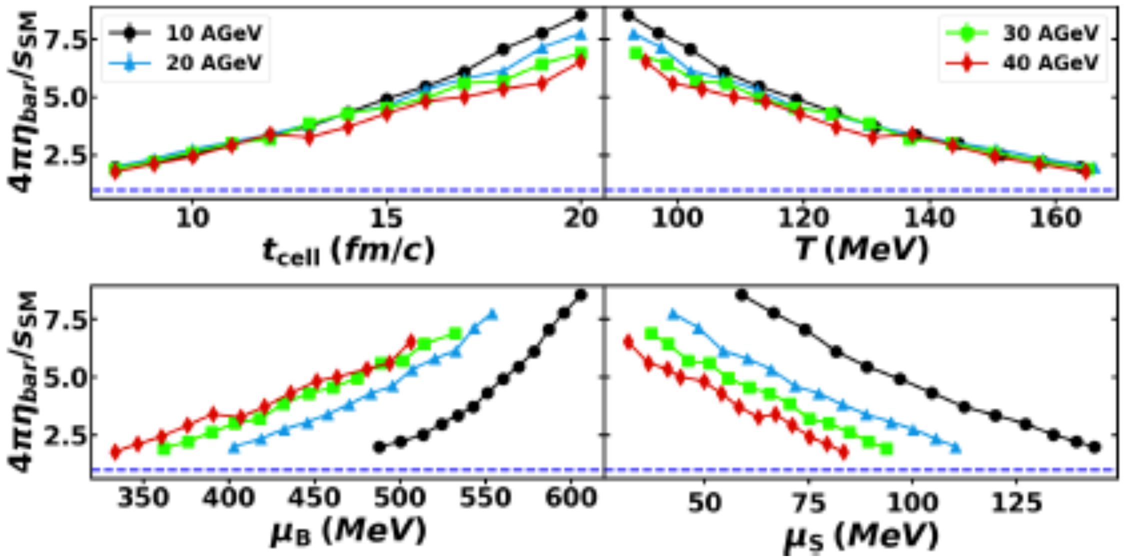

All hadrons

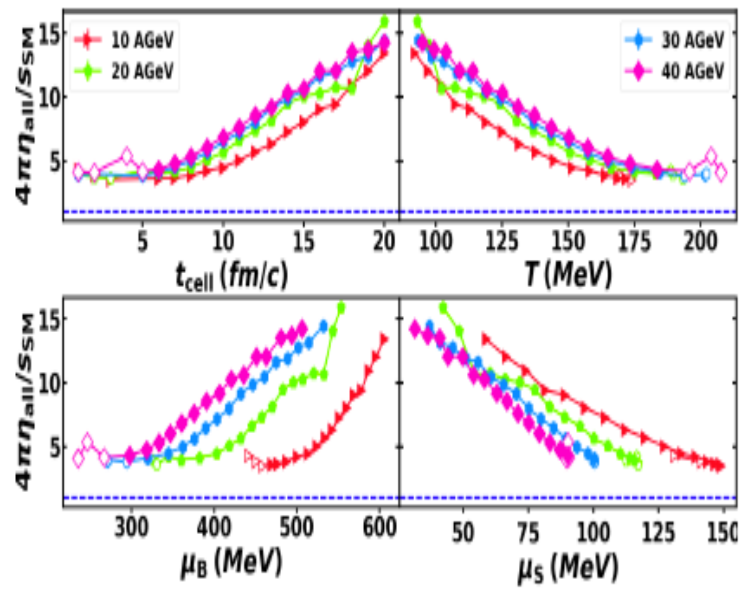

Mesons

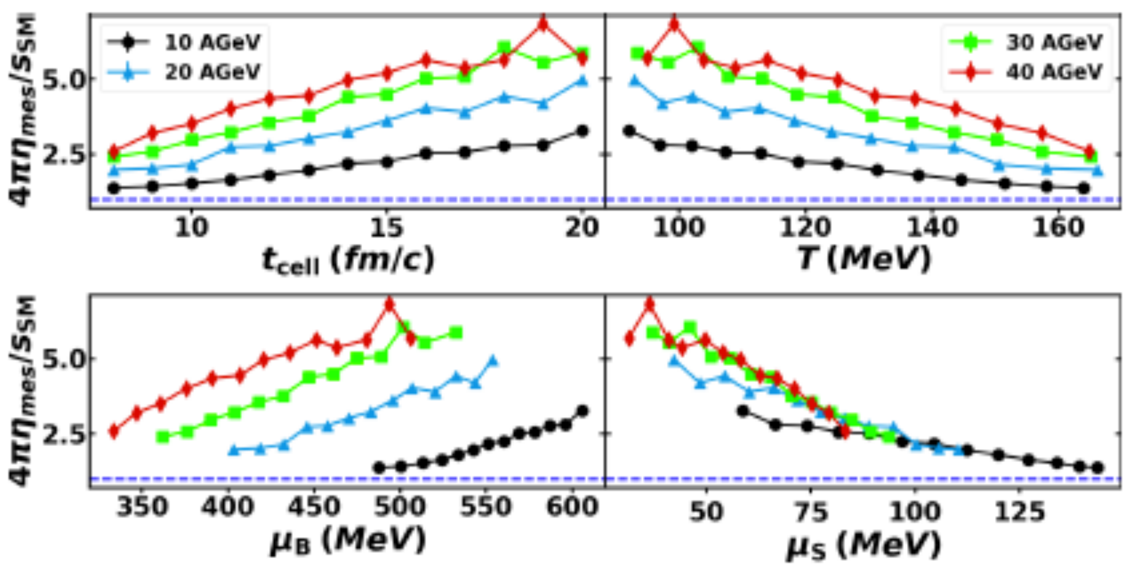

Reduction of the ratio $\frac{\eta}{s}$ with decreasing $\sqrt{s}$ is caused by the reduced contribution of mesons

CONCLUSIONS

Our study indicates that

- *total shear viscosity of hot and dense nuclear matter in the central cell drops with time for all four energies (10, 20, 30, 40 AGeV)*
- *after* $t \approx 6 \div 7$ *fm/c* η_{all} *in the cell is similar for all 4 energies*
- *the lower the beam energy, the lower the* η_M *and the higher the* η_B
- *partial shear viscosity of nucleons (pions) increases (decreases) with the drop of bombarding energy, whereas partial shear viscosities of kaons and* $\Lambda + \Sigma$ *are almost insensitive to the beam energy within the investigated interval*
- *the ratio of shear viscosity to entropy density* $\frac{\eta}{s}$ *also decreases with the energy drop. This decrease is attributed to mesons.*

Back-up

Slides

Shear viscosity

Newton:

$$T_{xy} = -\eta \frac{\partial u_x}{\partial y}$$

acts to reduce velocity gradients

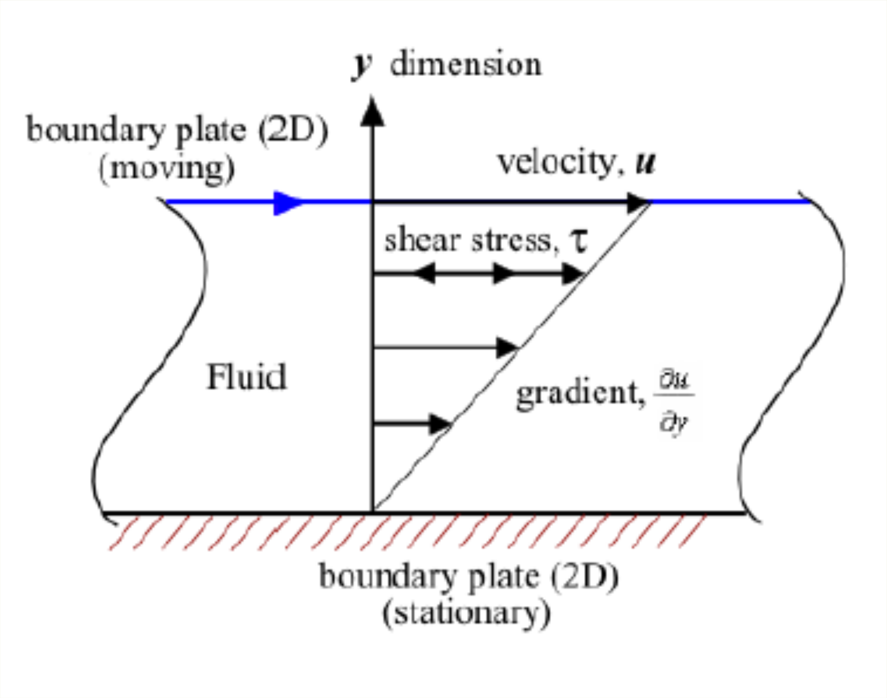

in closed system: energy conserved

kinetic energy gets converted to internal energy

$\Rightarrow$ dissipation

Comparison with other models

J.-B.Rose et al., PRC 97(2018) 055204

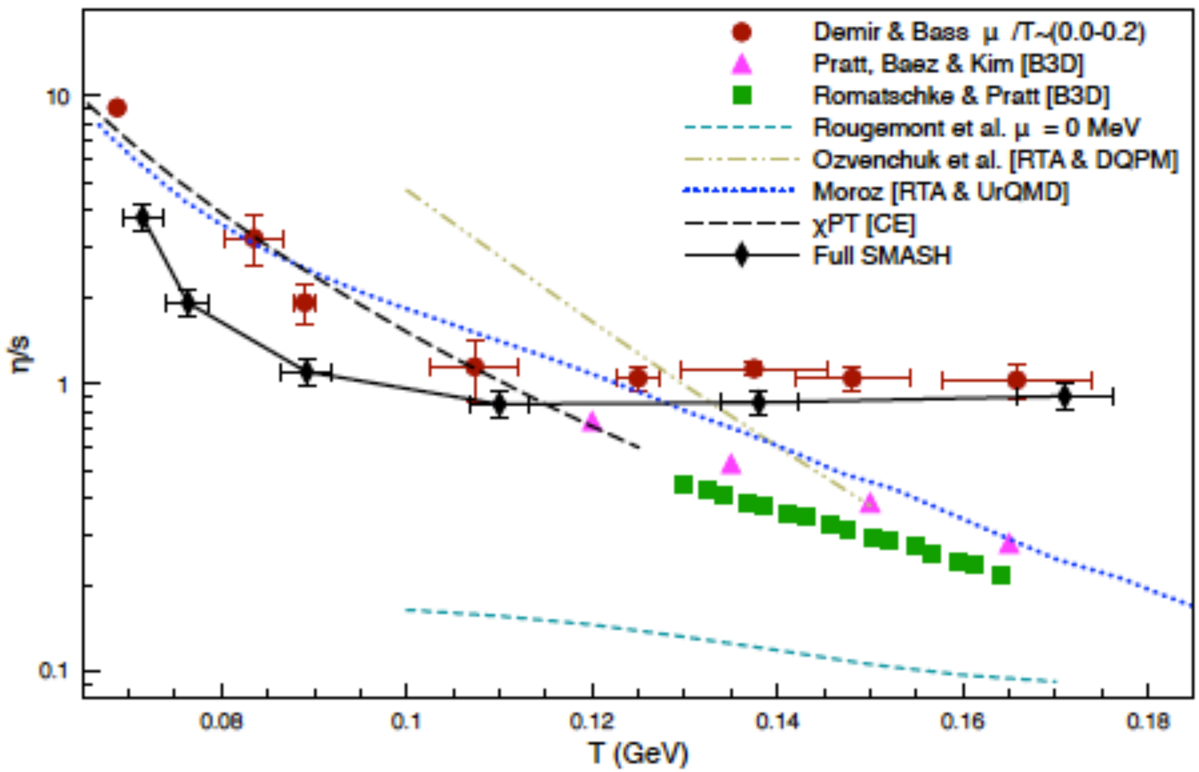

Comparison of different model predictions for the hadron gas η/s at $\mu_B = 0$

Entropy density of nonequilibrium state

Entropy density

$$s = -\sum_i \frac{g_i}{(2\pi\hbar)^3} \int_0^\infty f_i(p, m_i)\ [\ln f_i(p, m_i) - 1]\ d^3p$$

Microscopic distribution function

$$f_i^{\text{mic}}(p) = \frac{(2\pi\hbar)^3}{V g_i} \frac{dN_i}{d^3p}$$

Results: $\eta/s_{noneq.}$

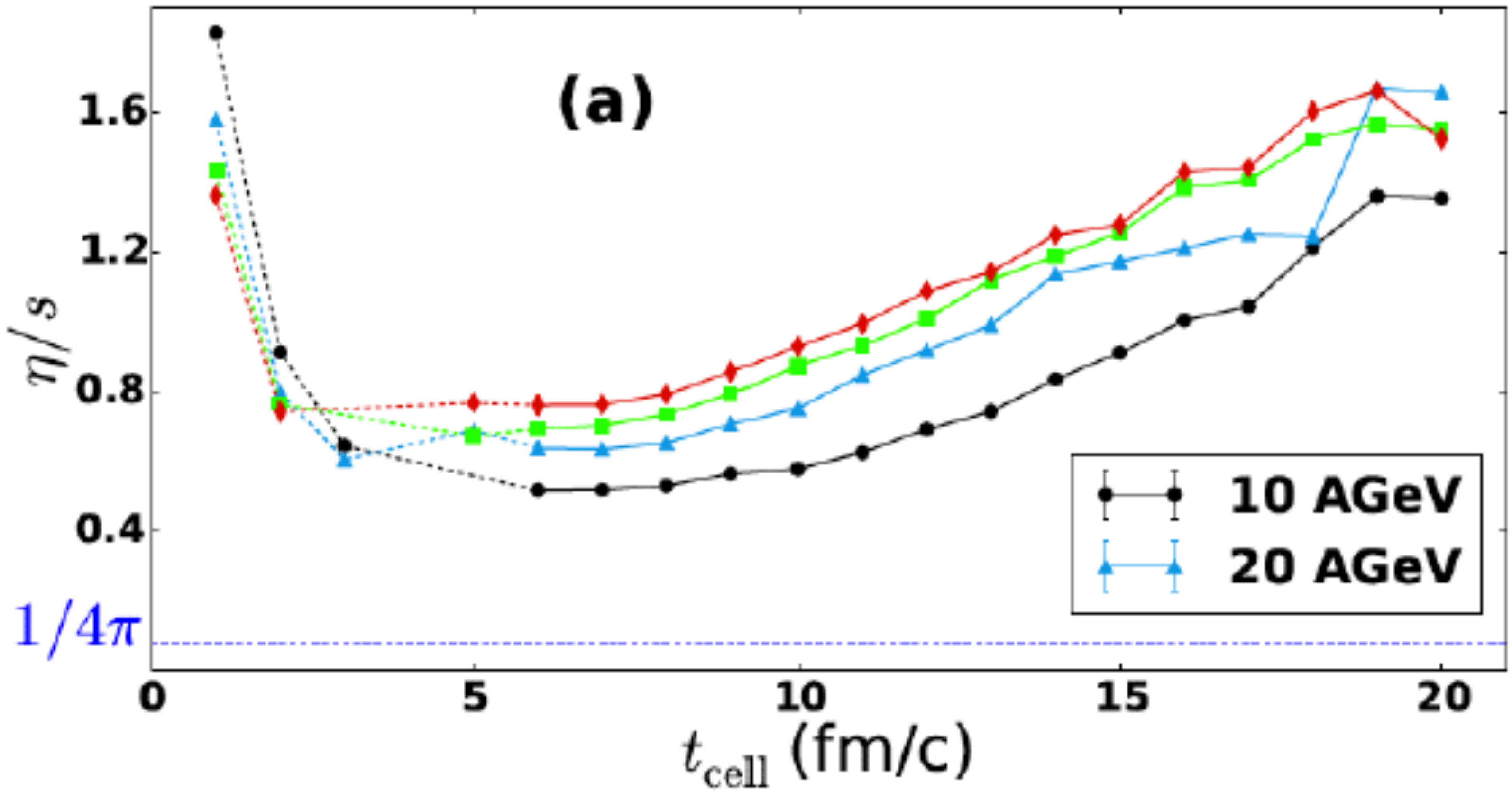

- Dynamics of $\eta/s_{noneq.}$ in cell
- η/s drops with time for $t_{\rm cell} \leq 6$ fm/c. Then it increases for all four energies
- Pronounced minima for all reactions